International Journal of GEOMATE
(Geotechnique, Construction Materials and Environment)
ISSN: 2186-2982 (P), 2186-2990 (O), Japan
Vol. 31, Issue 144, August, 2026, pp.131-140; DOI: 10.21660/2026.144.5533

EFFECT OF POLYPROPYLENE FIBER LENGTH ON RHEOLOGY, FROST RESISTANCE, PHASE COMPOSITION AND MICROSTRUCTURE OF SILICA FUME-MODIFIED SELF- COMPACTING CONCRETE

*Assel Ospanova[1], Daniyar Akhmetov[1], Evgeniya Tkach[2], Bagdat Uskembayeva[1], Bakytkul Aubakirova[3], Yerlan Auyesbayev[4] , Inna Kolesnikova[5]

[1]Satbayev University, Republic of Kazakhstan; [2]National Research Moscow State Civil Engineering University, Moscow, Russia; [3]Kozybayev University, Republic of Kazakhstan; [4]Caspian University , Republic of Kazakhstan ; [5]International Education Corporation, Republic of Kazakhstan

*Corresponding Author, Received: 12 March 2026, Revised: 08 May 2026, Accepted: 26 May 2026

ABSTRACT: Self-compacting concrete (SCC) incorporating silica fume is characterized by a dense microstructure and reduced permeability; however, the influence of polypropylene fiber length on simultaneously ensuring self-compactability and frost resistance remains insufficiently investigated. The objective of this study was to evaluate the effect of low-modulus polypropylene fiber length (6–20 mm) on the rheological behavior, durability performance, and microstructure of SCC. The mixture composition and superplasticizer dosage were kept constant; only the fiber length was varied at a fixed dosage of 1.0 kg/m³. Rheological properties were assessed using slump flow, T500 time, V-funnel, L-box, and J-ring tests. Durability was evaluated in terms of water absorption and frost resistance, while phase composition and morphology were analyzed by X-ray diffraction (XRD) and scanning electron microscopy (SEM), respectively. The results indicate that increasing fiber length led to reduced flowability of the mixture: slump flow decreased from 700 to 600 mm, T500 time increased from 2.1 to 5.8 s, V-funnel flow time increased from 6.3 to 13.8 s, the L-box ratio decreased from 1.00 to 0.82, and the J-ring blocking step increased from 8 to 26 mm. The optimal combination of properties was achieved at a fiber length of 12–15 mm, at which water absorption decreased to 4.1–4.2%, and frost resistance reached F350 (compared to 4.8% and F300 for the control mixture). XRD analysis did not reveal the formation of new crystalline phases, while SEM observations indicated the development of a dense fiber–matrix interfacial transition zone. The findings substantiate the suitability of 12–15 mm polypropylene fibers for achieving a balanced combination of rheological performance, durability, and service-related properties in silica fume-modified SCC under the tested conditions.

Keywords: Self-Compacting Cconcrete; Silica Fume; Polypropylene Fiber Length; Rheology; Freeze–Thaw Resistance; Water Absorption; SEM/XRD Analysis

1. INTRODUCTION

Modern construction is increasingly focused on reducing the carbon footprint while maintaining the durability of reinforced concrete structures. The cement industry remains one of the major sources of CO_2 emissions, accounting for approximately 7–8% of global anthropogenic emissions. Therefore, the partial replacement of cement with pozzolanic mineral admixtures is considered a key strategy for both decarbonization and enhancement of concrete performance [1].

One of the most promising materials in this context is self-compacting concrete (SCC), an innovative type of high-performance concrete developed by Okamura and Ouchi in the late 1980s at the University of Tokyo [2–4]. SCC is capable of consolidating under its own weight without external vibration, ensuring effective filling of formwork even in densely reinforced sections. However, the elevated content of cement and fine particles typically required for SCC increases both its cost and carbon footprint [5].

The relevance of incorporating industrial by-products and active mineral admixtures (SCMs/ACMs) into cementitious composites as a key pathway toward sustainable and low-carbon construction has been confirmed by recent review studies [6,7]. Accordingly, improving the efficiency and environmental performance of SCC through the use of mineral additives such as silica fume, zeolite, fly ash, metakaolin, and slag has become a research

priority, as these materials contribute to improved microstructure and long-term performance [6,8–10].

In studies conducted by Akhmetov et al., the influence of low-modulus polypropylene fiber on the mechanical and deformation characteristics of silica fume-modified SCC was investigated. It was demonstrated that an optimal selection of fiber length and dosage enhances flexural strength and crack resistance while reducing shrinkage deformation. The best overall performance was achieved with fibers approximately 12–15 mm in length at a dosage of 1–1.5 kg/m³ [11].

In SCC mixtures, silica fume serves not only as a partial cement replacement but also significantly influences the formation of the cementitious matrix. Through pozzolanic reactions and the microfiller effect, silica fume contributes to matrix densification, reduced porosity, and enhanced durability [12,14].

The combined use of silica fume and polypropylene fiber can be considered complementary in action: silica fume increases the density and homogeneity of the cement matrix, while fibers restrict the development of shrinkage-induced microcracks and improve resistance to crack propagation under flexural loading. These synergistic effects may influence not only the rheological behavior of fresh SCC mixtures but also the freeze– thaw resistance and microstructural characteristics of hardened concrete.

Despite the available data on strength and shrinkage performance, the rheological behavior of silica fume-modified SCC incorporating polypropylene fibers of different lengths, as well as the relationship between fiber length, freeze–thaw resistance, and microstructural evolution, remains insufficiently addressed. In particular, a comprehensive evaluation of flowability and passing ability (slump flow, V-funnel, L-box, J-ring), durability under cyclic freezing and thawing, and phase composition and morphology of hydration products supported by SEM observations and X-ray diffraction analysis is required [22,24–26].

Considering previously published results on the mechanical and deformation characteristics of silica fume-modified SCC reinforced with polypropylene fibers, and the identified effectiveness of fibers of optimal length, the present study represents a logical continuation of this research. It aims to provide an extended assessment of rheological performance, freeze–thaw resistance, and microstructural characteristics (SEM, XRD) in order to develop a more comprehensive understanding of the combined effect of the “silica fume + polypropylene fiber” system on the service performance and durability of self-compacting concrete.

2. RESEARCH SIGNIFICANCE

The present study is aimed at improving the service performance of silica fume-modified self-compacting concrete through optimization of polypropylene fiber length. Unlike previous studies mainly focused on mechanical and shrinkage behavior, the present research provides a comprehensive evaluation of rheological performance, freeze–thaw resistance, water absorption, phase composition, and microstructural characteristics of SCC reinforced with polypropylene fibers of different lengths. The results indicate that a rational selection of low-modulus synthetic fiber length makes it possible to maintain the self-compactability of the mixture while simultaneously enhancing durability parameters. The obtained results may be applied in the design of reinforced concrete structures and precast elements operating under cyclic freezing–thawing conditions. The proposed approach contributes to improved structural reliability and durability, reduced maintenance costs, and more efficient utilization of self-compacting concrete in infrastructure construction.

3. MATERIALS AND METHODS

3.1 Raw materials

Portland cement CEM II 42.5 trade name “Standard”, was used as the primary binder. Laboratory testing confirmed that its physical and mechanical properties complied with standard requirements. The residue on the 0.08 mm sieve was 0.5%, indicating high fineness, while the standard consistency of the cement paste was 28%. The compressive strength at 7 days reached 63 MPa and the flexural strength was 6.6 MPa. No violations of volume stability were observed [16,17]. The composition of cement clinker (Composition of cement clinker) and the chemical composition of Portland cement (Chemical composition of slag-portland cement) are presented in Tables 1 and 2.

Table 1. Composition of cement clinker

Name of components	Amount, %
The total content of tricalcium and bicalcium silicates (C_3S, C_2S)	75
Mass ratio of calcium to silicon oxide (CaO/SiO_2)	2.8
Magnesium oxide (MgO)	1.6

Table 2. Chemical composition of slag-portland cement

Name of components	Amount, %
Mass loss during calcination	0.7
Insoluble residue	1.4
Sulfur oxide (SO_3)	2.2
Magnesium oxide (MgO)	1.6
Chloride-ion (Cl^-)	0.05

Silica fume MK-95 produced by Tau-Ken Temir LLP (Karaganda, Republic of Kazakhstan) was used as a mineral admixture. The material contained 95.9% active SiO_2 and consisted of spherical particles with an average diameter of about 0.1 μm and a bulk density of 150–250 kg/m³. Its physicochemical properties meet the requirements for use in concrete mixtures [18–20]. The total binder consisted of Portland cement and silica fume, where silica fume replaced 10% of cement by mass in all mixtures. The total binder content was 594 kg/m³, and the water-to-binder ratio (w/b) was maintained at 0.44 for all mixtures.

Table 3. Chemical composition of silica fume MK-95, %

SiO_2	C	Moisture	Fe_2O_3	Al_2O_3	CaO	pH	ρ g/cm³	Loss on ignition
95.9	1.3	1.07	0.07	0.2	0.46	7.89	0.44	2.68

Quartz sand from the Giada LLP quarry was used as the fine aggregate. The sand had a fineness modulus of 2.3 (medium-grained), a moisture content of 2.5%, and a dust and clay content of 0.15%. The bulk density was 1140 kg/m³. The selected medium-grained quartz sand with a fineness modulus of 2.3 provided adequate particle packing, improved flowability, and reduced the risk of segregation in self-compacting concrete mixtures.

Crushed stone fractions of 5–10 mm and 10–20 mm produced by Ozentas were used as coarse aggregates. The content of flaky and elongated particles did not exceed 10%, while the mass loss after crushing was 1.28%. The bulk density was approximately 1240 kg/m³ [21].

The particle size distribution of fine and coarse aggregates was selected to ensure continuous grading and adequate packing density in accordance with EFNARC recommendations for self-compacting concrete. The combined grading of aggregates was designed to achieve optimal flowability and minimize segregation and blocking effects.

The specific gravity of the quartz sand was approximately 2.65, with a water absorption of about 1.0–1.5%. The coarse aggregates exhibited a specific gravity of approximately 2.70 and water absorption in the range of 0.5–1.0%, which is typical for crushed stone materials used in concrete production.

The selected proportion of coarse aggregate was limited to ensure sufficient passing ability of the mixture, reduce internal friction, and maintain the self-compactability of SCC without external vibration.

The dosage of the polycarboxylate ether-based superplasticizer was fixed at 6.5 kg/m³ according to the optimized SCC composition reported by D.A. Akhmetov et al., ensuring stable self-compactability in accordance with EFNARC recommendations [11,22].

Table 4. Characteristics of the superplasticizer CHRYSO Fluid Optima 203

Parameter	Description
State	Liquid
Viscosity	1.040±0.02 g/cm³
Color	Dark brown
pH	6.00±1
Solid material	21.50±%5
Chloride content	< 0.10%
Alkali content	< 2.0%

Polypropylene fiber “FibraLux” was used as dispersed reinforcement. The monofilament fibers had a circular cross-section, a length of 6–20 mm, and a diameter of approximately 34 μm. The surface was treated with Silastol CUT 70 to improve dispersion and adhesion to the cement matrix.

The fiber density was 0.91 g/cm³, with tensile strength of 320–600 MPa, elastic modulus of 3500–3900 MPa, and elongation at break up to 200%. The fibers exhibited negligible water absorption and thermal stability up to 160–170 °C [23].

The aspect ratio ranged from approximately 176 to 588 depending on fiber length, influencing rheological behavior and fiber–matrix interaction. At a dosage of 1.0 kg/m³, the mixture contained about 12.9 million fibers per cubic meter, ensuring uniform dispersion and crack-bridging.

The fiber dosage was fixed at 1.0 kg/m³ based on the optimized SCC composition reported by Akhmetov et al. [11], ensuring stable self-compactability, uniform dispersion, and the absence of blocking effects in accordance with EFNARC recommendations.

The composition of the self-compacting concrete used in the present study was adopted based on a previously developed and validated

mixture reported by Akhmetov et al. [11]. Within the framework of this research, the specified composition was used as the reference matrix, and the experimental program was aimed at evaluating the effect of polypropylene fiber length on rheological performance, freeze–thaw resistance, microstructural characteristics and phase composition.

Table 5. Concrete mixture composition

Mixture designation	Control mix	F6	F12	F15	F18	F20
Fiber length, mm	-	6	12	15	18	20
Cement, kg/m³	540	540	540	540	540	540
Sand, kg/m³	944	944	944	944	944	944
Crushed stone 5–10 mm, kg/m³	625	625	625	625	625	625
Crushed stone 10–20 mm, kg/m³	175	175	175	175	175	175
Silica fume, kg/m³	54	54	54	54	54	54
Fiber, kg/m³	0	1.0	1.0	1.0	1.0	1.0
Super plasticizer, kg/m³	6.5	6.5	6.5	6.5	6.5	6.5
Water, kg/m³	260	260	260	260	260	260

All mixtures were prepared under the same laboratory conditions using the mixture proportions presented in Table 5. The ambient laboratory temperature during mixing and casting was maintained at 20 ± 2 °C. The control mixture contained silica fume without polypropylene fiber, whereas the fiber-reinforced mixtures differed only in polypropylene fiber length; the fiber dosage, cement content, silica fume content, aggregate composition, water-to-binder ratio and superplasticizer dosage were kept constant. The dry components, including cement, silica fume, sand and coarse aggregates, were first mixed until a visually homogeneous mixture was obtained. Water premixed with the polycarboxylate-based superplasticizer was then gradually added, followed by gradual introduction of polypropylene fibers to reduce fiber balling and ensure uniform dispersion within the cementitious matrix. The total mixing time was approximately 5–7 minutes, including initial dry mixing (2 minutes) and subsequent mixing after water and superplasticizer addition (3–5 minutes). No external vibration was applied during casting, since the mixtures were designed as self-compacting concrete. The fresh mixture was placed into molds under its own weight. The specimens were kept in molds for 24 h under protected conditions to prevent moisture loss, then demolded and cured in water at 20 ± 2 °C until the testing age. For each mixture and each test type, at least three specimens were prepared and tested. The experimental results are reported as mean values with standard deviations, where applicable, to characterize the variability of the measurements. The same mixing, casting and curing procedure was applied to all compositions to ensure comparability of the results.

3.2 Test Methods

The rheological properties of the self-compacting concrete mixtures were evaluated in accordance with the EN 12350 series of European standards and EFNARC recommendations. The test program included slump flow diameter and T500 time for assessing filling ability and viscosity, V-funnel flow time, L-box ratio, and J-ring blocking step for evaluating passing ability and resistance to blocking of SCC mixtures. Slump flow and T500 were used to determine the deformability and flow rate of the mixtures, while the V-funnel, L-box, and J-ring tests were used to evaluate viscosity, passing ability, and resistance to blocking under conditions simulating reinforcement congestion. All tests were conducted at a temperature of 20 ± 2 °C. Each measurement was performed at least three times, and the reported results represent average values [24–26].

Fig. 1. Rheological testing of SCC: (a) L-box test; (b) V-funnel test

Freeze–thaw resistance was determined according to GOST 10060–2012 using cyclic freezing and thawing of fully water-saturated cubic specimens (100 × 100 × 100 mm). Prior to testing,

the specimens were saturated with water to constant mass. The specimens were frozen at −18 ± 2 °C and thawed in water at +20 ± 2 °C. The frost resistance grade was established based on mass loss and residual compressive strength after repeated freeze–thaw cycles, provided that the reduction in strength and mass did not exceed the permissible limits specified by the standard [27].

Water absorption was determined according to GOST 12730.3–2020 using cubic specimens (100 × 100 × 100 mm). The specimens were first dried to constant mass at 105 ± 5 °C, cooled to room temperature, and then immersed in water until constant saturated mass was reached. Water absorption was calculated as the relative increase in mass after saturation and expressed as a percentage [28].

X-ray diffraction (XRD) analysis was performed for two representative self-compacting concrete compositions: the control mixture with silica fume (SCC + SF) and the mixture with silica fume and 12 mm polypropylene fiber (SCC + SF + F12). These mixtures were selected because all compositions had the same cementitious matrix, silica fume content, water-to-binder ratio, aggregate composition, superplasticizer dosage and fiber dosage; only the polypropylene fiber length was varied. The F12 mixture was selected as the representative fiber-reinforced composition because it showed the most balanced rheological, mechanical and durability-related performance under the tested conditions.

The analyses were conducted using a modernized automated DRON-3 X-ray diffractometer with CuKα radiation and a β-filter operating at 35 kV and 20 mA. Diffraction patterns were recorded in θ–2θ scanning mode at a scanning rate of 2°/min. Prior to analysis, the samples were ground to a particle size of less than 0.05 mm.

Phase identification and semi-quantitative evaluation were carried out using the ICDD PDF-2 database, Release 2022, and HighScore Plus software. The crystalline phase content was estimated using the reference intensity ratio (RIR) method. The method provides semi-quantitative results with an estimated error of 10–20% for phases exceeding 10 wt.%, while minor phases were identified qualitatively. Since C–S–H gel is poorly crystalline or amorphous, it cannot be accurately quantified by conventional XRD. Therefore, the XRD results were used mainly to identify dominant crystalline phases and were interpreted as representative rather than as a complete phase-composition assessment of all fiber lengths. Since XRD was performed only for the control and F12 mixtures, the results were not generalized to all fiber lengths.

Microstructural analysis was performed using scanning electron microscopy (SEM) on selected representative specimens. The SEM examination focused on the control mixture and the F12 mixture, since the matrix composition was identical for all mixtures and only the fiber length was varied. The purpose of SEM analysis was to support the interpretation of performance trends by examining fracture morphology, pore structure, microcracks and fiber–matrix interaction.

Fragments approximately 1–2 cm in size were collected after mechanical testing, cleaned of surface dust, and mounted on aluminum stubs, Ø12/25 mm, using conductive carbon tape without epoxy impregnation or conductive coating. SEM observations were conducted in low-vacuum mode to examine dielectric materials without additional coating and to minimize charging effects. Imaging was performed in secondary electron (SE) mode at magnifications of ×2000–×4000.

The SEM images were interpreted qualitatively as supporting evidence for the mechanical and durability results. Since no quantitative image analysis of porosity or interfacial transition zone thickness was performed, the SEM results were discussed using cautious terminology such as “SEM observations indicated” and “SEM images suggested” rather than as definitive confirmation.

4. RESULTS AND DISCUSSION

4.1 Rheological, Physical and Durability Properties of Self-Compacting Concrete

Table 6 showed the fresh-state and rheological properties of the self-compacting concrete mixtures modified with polypropylene fibers of different lengths were evaluated using slump flow, T500 time, fresh density, V-funnel, L-box and J-Ring tests in accordance with EFNARC recommendations.

Table 6. Fresh-state properties of self-compacting concrete mixtures

Mixture designation	Control mix	F6	F12	F15	F18	F20
Slump flow, mm	700	675	630	624	615	600
T500, s	2.1	2.8	3.6	3.9	4.5	5.8
V-funnel flow,s	6.3	7.4	9.0	9.6	10.5	13.8
L-box (h_2/h_1)	1.00	0.98	0.96	0.95	0.94	0.82
J-Ring, $\Delta D = D_o - D_j$ (mm)	8	10	16	18	22	26

Fresh density, kg/m³	2390	2395	2343	2340	2336	2325

**Values are presented as mean ± standard deviation (n = 3).*

These tests make it possible to assess the filling ability, viscosity, passing ability and resistance to blocking of SCC mixtures. The obtained experimental results are presented in Table 6.

The fresh-state properties of self-compacting concrete were noticeably influenced by the length of polypropylene fiber. The control mixture showed the highest slump flow value of 700 mm, the shortest T500 time of 2.1 s, and a fresh density of 2390 kg/m³. With increasing fiber length, the slump flow gradually decreased from 675 mm for F-6 to 600 mm for F-20, while the T500 time increased from 2.8 s to 5.8 s, indicating reduced filling ability and increased viscosity of the mixtures.

According to EFNARC classification, the control mixture and F-6 corresponded to the SF2 class, while F-12, F-15, F-18 and F-20 corresponded to the SF1 class. The fresh density of the fiber-reinforced mixtures ranged from 2325 to 2343 kg/m³.

Compared with the control mixture without fiber (V-funnel flow time – 6.3 s, L-box ratio – 1.00, J-Ring ΔD – 8 mm), the incorporation of 6 mm fibers caused a slight reduction in flowability and passing ability; however, the obtained values remained within the acceptable limits for SCC.

For mixtures containing 12–15 mm fibers, the V-funnel flow time increased to 9.0–9.6 s and J-Ring ΔD increased to 16–18 mm, while satisfactory L-box ratios (0.95–0.96) were maintained. This indicated preservation of self-compacting ability without significant blocking effects.

Further increasing the fiber length to 18–20 mm resulted in a considerable increase in T500 time (4.5–5.8 s), flow time (10.5–13.8 s), a decrease in the L-box ratio to 0.82–0.94, and an increase in J-Ring ΔD to 22–26 mm. These results indicated reduced self-compactability and a higher tendency toward blocking.

The fiber dosage of 1.0 kg/m³ was selected based on preliminary trials and previous studies, which showed that this dosage provided effective crack control without excessive loss of workability. Three specimens were tested for each mixture, and the average values are presented in the tables. Freeze–thaw resistance was determined according to GOST 10060–2012 using cyclic freezing and thawing in water. Water absorption was measured according to GOST 12730.3–2020.

The frost resistance and water absorption of the studied self-compacting concrete mixtures were significantly affected by polypropylene fiber length (Table 7). The control mixture showed 4.8% water absorption, 2.6% mass loss after freeze–thaw cycles, 87.2% residual compressive strength, and frost resistance grade F300.

Table 7. Frost Resistance and Water Absorption of SCC Mixtures

Mixture designation	**Control mix**	**F6**	**F12**	**F15**	**F18**	**F20**
Water absorption, %	4.8	4.5	4.1	4.2	4.3	5.2
Mass loss after freeze–thaw, %	2.6	2.1	1.4	1.6	1.9	2.3
Residual compressive strength, %	87.2	89.1	93.4	92.6	90.3	85.6
Frost resistance grade	F300	F300	F350	F350	F300	F250

**Values are presented as mean ± standard deviation (n = 3).*

The addition of 6 mm fibers slightly improved durability, reducing water absorption to 4.5% and mass loss to 2.1%, while increasing residual compressive strength to 89.1%, with frost resistance remaining at F300.

The best results were obtained for mixtures with 12–15 mm fibers, which showed the lowest water absorption (4.1–4.2%), minimal mass loss (1.4–1.6%), and the highest residual compressive strength (92.6–93.4%), corresponding to frost resistance grade F350. This was attributed to improved matrix densification, reduced capillary porosity, and effective crack-bridging by the fibers.

Further increasing fiber length to 18–20 mm led to higher water absorption (4.3–5.2%), greater mass loss (1.9–2.3%), and lower residual compressive strength (85.6–90.3%), resulting in reduced frost resistance (F300–F250). This suggests that excessive fiber length may reduce mixture homogeneity and negatively affect durability-related properties.

Thus, under the investigated conditions, polypropylene fibers with a length of 12–15 mm were the most effective for improving frost resistance and durability of silica fume-modified self-compacting concrete.

4.2 X-ray Diffraction Results

X-ray diffraction analysis was performed for two representative mixtures: the control mixture (SCC + SF) and the mixture containing 12 mm polypropylene fiber (SCC + SF + F12). These

compositions were selected because all mixtures had the same binder system and mineral base, differing only in fiber length, while F12 showed the most balanced combination of rheological, durability and microstructural performance under the tested conditions.

The XRD measurements were carried out using a DRON-3 diffractometer with CuKα radiation at 35 kV and 20 mA. Phase identification was performed using the ICDD PDF-2 database (Release 2022) and HighScore Plus software. Since bulk XRD patterns are mainly dominated by aggregate minerals, while cement hydration products are largely amorphous, the analysis was used primarily for comparative evaluation of representative mixtures.

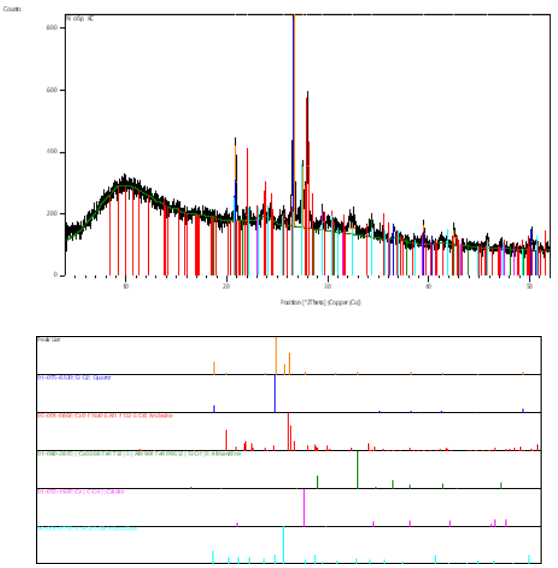

Fig. 2. X-ray diffraction pattern of the control mixture.

A pronounced amorphous hump is observed in the diffraction pattern within the 2θ range of approximately 20–35°, which is characteristic of gel-like hydration products of cement (C–S–H), as well as amorphous silica involved in the pozzolanic reaction. Against this background, intense diffraction peaks of quartz (SiO_2) are detected, with the main reflection at 2θ ≈ 26.6°, along with peaks corresponding to feldspars, attributable to the presence of natural aggregates.

Additionally, moderate reflections of calcite ($CaCO_3$) are identified, associated with carbonation processes occurring in the cement matrix.

Semi-quantitative X-ray diffraction analysis showed that the phase composition of the specimen is dominated by quartz (SiO_2) (~50%), originating from natural aggregates. Feldspar minerals, including sodium–calcium feldspar ($Ca_{0.4}Na_{0.6}Al_{1.4}Si_{2.6}O_8$) (~26%) and potassium feldspar ($KAlSi_3O_8$) (~11%), are also present and are associated with the mineral composition of the aggregates rather than cement hydration.

Table 8. Results of semi-quantitative analysis of crystalline phases in the control mixture

№ PDF cards	Chemical formula	Mineral	Concentration, %
01-075-8320	SiO_2	Quartz	50
05-001-0864	$Ca_{0.4}Na_{0.6}Al_{1.4}Si_{2.6}O_8$	Feldspar	26
01-080-2815	$(Ca_{0.268}Fe_{0.732})_3(Al_{0.904}Fe_{0.096})_2(SiO_4)_3$	Garnet (almandine)	6
01-072-1937	$Ca(CO_3)$	Calcite	7
00-001-0705	$KAlSi_3O_8$	Potassium feldspar	11

Calcite ($CaCO_3$) (~7%) was identified as a carbonation product of the cement matrix, while minor almandine ($(Ca,Fe)_3(Al,Fe)_2(SiO_4)_3$) (~6%) originates from the aggregates. Overall, the phase composition is typical for cementitious composites containing natural aggregates, with the cement matrix structure mainly governed by amorphous hydration products.

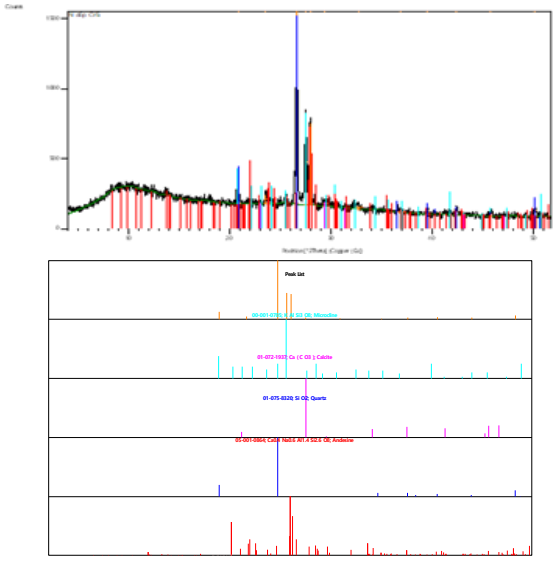

Fig. 3. X-ray diffraction pattern of SCC + SF + F12.

The X-ray diffraction pattern of the self-compacting concrete modified with silica fume and polypropylene fiber shows the presence of both amorphous and crystalline components. A broad amorphous hump in the 2θ range of 20–35°

indicates the predominance of C–S–H gel and the participation of amorphous silica fume in the pozzolanic reaction. The crystalline phases are mainly represented by quartz (SiO_2) with a characteristic peak at 2θ ≈ 26.6° and feldspar minerals originating from the aggregates, while weak reflections of calcite ($CaCO_3$) indicate carbonation of the cement matrix. No new crystalline phases were detected after the incorporation of polypropylene fiber, which suggests that the main structural development of the concrete is governed by cement hydration and the pozzolanic reaction of silica fume.

Table 9. Results of semi-quantitative analysis of crystalline phases in SCC + SF + F12

№ PDF cards	Chemical formula	Mineral	Concentration, %
00-001-0705	$KAlSi_3O_8$	Potassium feldspar	20
01-072-1937	$Ca(CO_3)$	Calcite	2
01-075-8320	SiO_2	Quartz	58
05-001-0864	$Ca_{0.4}Na_{0.6}Al_{1.4}Si_{2.6}O_8$	Feldspar	20

Semi-quantitative XRD analysis suggested that the phase composition is dominated by quartz (SiO_2) (~58%) originating from aggregates. Feldspar minerals, including potassium feldspar ($KAlSi_3O_8$) (~20%) and sodium–calcium feldspar ($Ca_{0.4}Na_{0.6}Al_{1.4}Si_{2.6}O_8$) (~20%), were also observed and are associated with the aggregate composition rather than cement hydration. Calcite ($CaCO_3$) (~2%) was detected as a carbonation product of the cement matrix. The cementitious matrix is mainly governed by amorphous hydration products.

Due to the predominance of crystalline aggregate phases and the amorphous nature of C–S–H, the XRD analysis is considered qualitative. The RIR-based phase contents should be interpreted with caution, particularly for phases below 10 wt.% and amorphous components; therefore, the results are used mainly for phase identification and comparative analysis.

4.3 Microstructural Investigation

The control self-compacting concrete mixture containing silica fume (SCC + SF) and the mixture modified with silica fume and 12 mm polypropylene fiber (SCC + SF + F12) were selected for microstructural investigation based on the results of comprehensive testing, which identified this fiber length as providing the optimal combination of rheological properties, freeze–thaw resistance, and water absorption.

Since all mixtures had the same mineral base and differed only in dispersed reinforcement parameters, the microstructural analysis was limited to representative specimens to characterize the cement matrix structure and the fiber–matrix interfacial zone while avoiding duplication of similar SEM images.

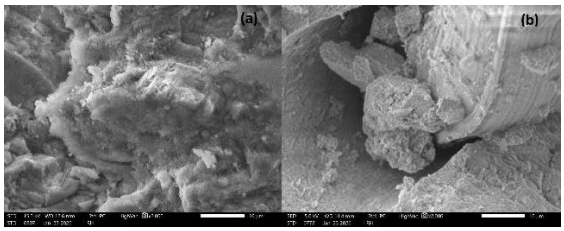

Fig. 4. SEM images at ×2000 magnification: (a) self-compacting concrete containing silica fume; (b) self-compacting concrete containing silica fume and 12 mm polypropylene fiber.

SEM observations of representative images suggested that the control mixture appeared to exhibit a heterogeneous cementitious matrix with a gel-like morphology and localized pore regions typical of silica fume-modified SCC.

In contrast, the mixture containing 12 mm polypropylene fiber appeared to show a more developed fiber–matrix interfacial zone, with fiber surfaces partially covered by hydration products and no clearly visible interfacial defects or debonding. The matrix in the vicinity of the fiber appeared denser.

These observations suggest differences in microstructural organization associated with fiber incorporation.

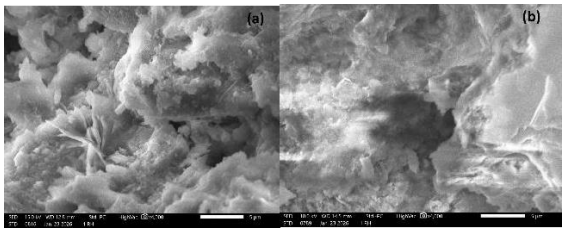

Fig. 5. SEM micrographs at ×4000 magnification:

(a) self-compacting concrete containing silica fume; (b) self-compacting concrete containing silica fume and 12 mm polypropylene fiber.

SEM observations at ×4000 magnification suggested a finely dispersed gel-like structure of cement hydration products, with localized plate-like and needle-like formations. The

microstructure appeared heterogeneous, with uneven distribution of hydrated phases and the presence of isolated micropores within the intergranular space.

The mixture modified with silica fume and 12 mm polypropylene fiber appeared to exhibit a more compact cementitious matrix, particularly near the fiber–matrix interfacial zone. Hydration products appeared more densely distributed in this region, and no clearly pronounced interfacial defects or debonding were observed.

Comparison of the microstructures at ×4000 magnification suggests differences in the distribution and morphology of hydration products after fiber incorporation, which may indicate the formation of a more organized interfacial zone.

The presented SEM micrographs are representative and were obtained under consistent imaging conditions with scale bars, as described in the Materials and Methods section. The SEM analysis is qualitative; therefore, the observations are discussed in terms of general trends rather than precise quantitative values.

5. CONCLUSION

Based on the conducted experimental investigations, the results indicated that the length of low-modulus polypropylene fiber affected the rheological performance, durability parameters, and microstructural organization of silica fume-modified self-compacting concrete.

An increase in fiber length from 6 to 20 mm resulted in a gradual reduction in the flowability of self-compacting concrete mixtures. The slump flow decreased from 700 mm to 600 mm, the T500 time increased from 2.1 s to 5.8 s, the V-funnel flow time increased from 6.3 s to 13.8 s, the L-box ratio decreased from 1.00 to 0.82, and the J-ring blocking step increased from 8 mm to 26 mm. Fibers with a length of 12–15 mm were found to provide a balanced rheological behavior, maintaining self-compactability without significant blocking effects.

Durability-related properties were also influenced by fiber length. The lowest water absorption values (4.1–4.2%) and the highest frost resistance grade (F350) were obtained for mixtures containing 12–15 mm fibers, compared with 4.8% water absorption and frost resistance grade F300 for the control mixture. Further increasing the fiber length to 18–20 mm was associated with higher water absorption, reduced frost resistance, and lower residual compressive strength, which suggested a decrease in mixture homogeneity and durability performance.

The X-ray diffraction results suggested that the incorporation of polypropylene fiber did not lead to the formation of new crystalline phases in the representative mixtures. The phase composition was mainly governed by quartz and feldspar minerals originating from the aggregates, while the cementitious matrix was associated with amorphous hydration products, including C–S–H gel, and the pozzolanic reaction of silica fume. Therefore, the effect of fiber reinforcement was mainly related to microstructural organization and the fiber–matrix interfacial zone rather than changes in crystalline phase composition.

SEM observations suggested the possible formation the formation of a developed fiber–matrix interfacial zone in the mixture containing 12 mm fibers. The fiber surfaces were partially covered with hydration products, and no pronounced interfacial defects or debonding were clearly observed, suggesting compatibility between the dispersed reinforcement and the densified silica fume-modified matrix.

Under the investigated conditions, for the mixture containing 1.0 kg/m³ of polypropylene fiber and 54 kg/m³ of silica fume, fibers with a length of 12–15 mm can be considered the most rational, as they provide a balanced combination of rheological performance, durability, and microstructural stability under cyclic freeze–thaw conditions. These findings are valid for the investigated mixture composition and may vary with changes in fiber dosage and binder composition.

6. REFERENCES

1. International Energy Agency (IEA), Cement, IEA, 2022. https://www.iea.org/reports/cement
2. Okamura H., Ouchi M., Self-compacting concrete, Journal of Advanced Concrete Technology, 1(1), 2003, pp.5–15. https://doi.org/10.3151/jact.1.5
3. Domone P. L., Self-compacting concrete: An analysis of 11 years of case studies, Cement and Concrete Composites, 28(2), 2006, pp.197–208. https://doi.org/10.1016/j.cemconcomp.2005.10.003
4. Domone P.L., A review of the hardened mechanical properties of self-compacting concrete, Cement and Concrete Composites, 29(1), 2007, pp.1–12. https://doi.org/10.1016/j.cemconcomp.2006.07.0 10

5. Sankar A. S., Hari R., Mini K. M., Effect of micro silica and aggregate size on cracking of self-compacting concrete, Proceedings of the Institution of Civil Engineers – Construction Materials, 173(5), 2020, pp.227–233. https://doi.org/10.1680/jcoma.18.00080
6. Moolchandani K., Industrial byproducts in concrete: A state-of-the-art review, Next Materials, 2025, 100330. https://doi.org/10.1016/j.nxmate.2025.100593
7. Memon N. A., Memon M. A., Lakho N. A., Memon F. A., Keerio M. A., Memon A. N., A review on self compacting concrete with cementitious materials and fibers, Engineering, Technology & Applied Science Research, 8(3), 2018,pp.2969-2974. https://doi.org/10.48084/ETASR.2006
8. Mehta P. K., Monteiro P. J. M., Concrete: Microstructure, Properties, and Materials, 4th ed., McGraw-Hill Education,2014.ISBN-13: 978-0-07-179787-0
9. Ofuyatan O. M., Adeniyi A. G., Ighalo J. O., Evaluation of fresh and hardened properties of blended silica fume self-compacting concrete, Research on Engineering Structures and Materials,2021. http://dx.doi.org/10.17515/resm2020.228ma1023
10. Vinod Kumar G., Narendra Kumar B., Effect on mechanical, durability and microstructural properties of high strength self-compacting concrete with inclusion of micro and nano silica, Materials Today: Proceedings, 60, 2022, pp.569–575. https://doi.org/10.1016/j.matpr.2022.02.064
11. Akhmetov D. A., Akhazanov S., Jetpisbayeva A., Pukharenko Y., Root Y., Utepov Y., Akhmetov A., Effect of low-modulus polypropylene fiber on physical and mechanical properties of self-compacting concrete, Case Studies in Construction Materials, 16, 2022, e00814. https://doi.org/10.1016/j.cscm 2022.e00814
12. Lothenbach B., Le Saout G., Gallucci E., Scrivener K., Influence of silica fume on the hydration of Portland cement, Cement and Concrete Research, 41(3), 2011, pp.301–310. https://doi.org/10.1016/j.cemconres.2010.11.010
13. Begentayev M. M., Kuldeyev E. I., Zhumadilova Z. O., Akhmetov D. A., Tolegenova A. K., Zhagifarov A. M., Nurlybayev R. E., Alikhan A., Investigation of waste-based self-compacting concrete: Analysis of rheology and hydration with silica fume and fly ash, ES Materials and Manufacturing, 28, 2025 https://www.espublisher.com/journals/articledeta ils/1498
14. Massana J., Reyes E., Bernal J., León N., Sánchez-Espinosa E., Influence of nano- and micro-silica additions on the durability of a high performance self-compacting concrete, Construction and Building Materials, 165, 2018, pp.93–103. https://doi.org/10.1016/j.conbuildmat.2017.11.08 6
15. Zhagifarov A., Talal A., Akhmetov D., Suzev N., Kolesnikova I., Effectiveness of road slabs produced using microsilica and fiber quality improvement, International Journal of GEOMATE, 28(126), 2025. https://doi.org/10.21660/2025.126.4335
16. GOST 31108–2003, Common cements. Specifications, Moscow: Standartinform, 2004.
17. GOST 10180–2012, Concrete. Methods for strength determination, Moscow: Standartinform, 2012.
18. EN 13263-1:2005+A1:2009, Silica fume for concrete — Part 1: Definitions, requirements and conformity criteria, Brussels: CEN, 2009.
19. ASTM C1240, Standard specification for silica fume used in cementitious mixtures, ASTM International, West Conshohocken, PA, USA.
20. Tau-Ken Temir STS LLP, Condensed microsilica. Technical specification No. 46976-1901-21-002, Karaganda, Republic of Kazakhstan, 2014.
21. GOST 32824–2014, Crushed stone and gravel from dense rocks for construction works. Specifications, Moscow: Standartinform, 2015.
22. EFNARC, The European Guidelines for Self-Compacting Concrete: Specification, Production and Use, Association House, Farnham, UK, 2005.
23. EN 14889-2:2006, Fibres for concrete — Part 2: Polymer fibres — Definitions, specifications and conformity, Brussels: CEN, 2006.
24. EN 12350-9:2010, Testing fresh concrete — Part 9: V-funnel test, Brussels: European Committee for Standardization (CEN), 2010.
25. EN 12350-10:2010, Testing fresh concrete — Part 10: L-box test, Brussels: European Committee for Standardization (CEN), 2010.
26. EN 12350-12:2010, Testing fresh concrete — Part 12: J-ring test, Brussels: European Committee for Standardization (CEN), 2010.
27. GOST 10060–2012, Concrete. Methods for determination of frost resistance, Moscow: Standartinform, 2013.
28. GOST 12730.3–2020, Concrete. Method for determination of water absorption, Moscow: Standartinform, 2020.